

**IMPACT CRATERS: WINDOWS THROUGH LAVA FLOWS IN OCEANUS PROCELLARUM.** S. Z. Weider<sup>1,2</sup>, I.A. Crawford<sup>1</sup> & K.H. Joy<sup>1,2</sup>, <sup>1</sup> Centre for Planetary Sciences, Birkbeck/UCL Research School of Earth Sciences, Gower Street, London, WC1E 6BT, UK. ([s.weider@ucl.ac.uk](mailto:s.weider@ucl.ac.uk)), <sup>2</sup>Space Science and Technology Department, Rutherford Appleton Laboratory, Didcot, Oxon, OX11 0QX, UK.

**Introduction:** Lunar mare basalts are made up of individual, compositionally and temporally, distinct lava flows [e.g. 1, 2]. Whilst the areal extent of these flows has often been remotely mapped [e.g. 1-5], determining their thickness and volume is more problematic. There are some depth estimates for the total basalt deposits [e.g. 6-8], but there are few such estimates for the individual lava flows [e.g. 9]. In this study we use Clementine multispectral reflectance data to identify conspicuous compositional signatures associated with the continuous ejecta of impact craters within an area of Oceanus Procellarum. These ejecta represent material excavated from older lava flows beneath that in which the craters are situated; their size can therefore be used to constrain the thicknesses of the surficial flows.

**Methods:** Clementine UV-Vis reflectance data were downloaded at full resolution (0.1 km/pixel) and in a simple cylindrical projection from the USGS Map-A-Planet website ([www.mapaplanet.org](http://www.mapaplanet.org)) as radiometrically, geometrically and photometrically controlled .raw files [10]. The files were extracted and analysed using an in-house IDL (Interactive Data Language) code. These data were used to produce maps of the study area in Oceanus Procellarum (Fig. 1) for various parameters, including FeO and TiO<sub>2</sub> wt. % abundances (according to the algorithms of [11] and [12] respectively).

**Results:** The TiO<sub>2</sub> wt. % abundance map reveals a number of craters within a particular lava flow ('P52', as termed by [2]) that appear to be surrounded by haloes of material with a lower TiO<sub>2</sub> content than the surrounding lava flow (see Fig. 2), and which approximate the extent of their continuous ejecta blankets (i.e. ~1 crater radius beyond the rim: [13, 14]). We hypothesize that these haloes evidence material that has been excavated from a lithology beneath the surface lava flow ('P52'), with a lower TiO<sub>2</sub> content. A candidate for this deeper lava flow is 'P24' (as termed by [2]), which is TiO<sub>2</sub>-poorer (by ~3 wt. %), and stratigraphically older than 'P52'.

Figure 3 is a plot of mean FeO and TiO<sub>2</sub> wt. % abundances for (i) the ejecta of the thirteen craters with TiO<sub>2</sub>-poor haloes identified in lava flow 'P52' and (ii) the average lava flow compositions of 'P52' and 'P24'. This figure illustrates that the ejecta of the thirteen haloed craters have a distinct composition from that of lava flow 'P52' in which they lie; the ejecta

compositions are more similar to that of the proposed underlying lava flow, 'P24'.

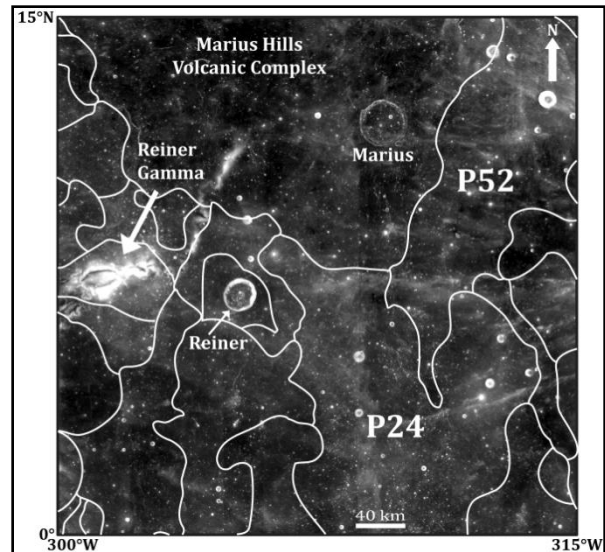


Figure 1. A Clementine 750 nm image of the study area within Oceanus Procellarum, showing the major surface features and lava flow boundaries (as mapped in [2]); lava flows relevant to this work, 'P24' and 'P52', are marked.

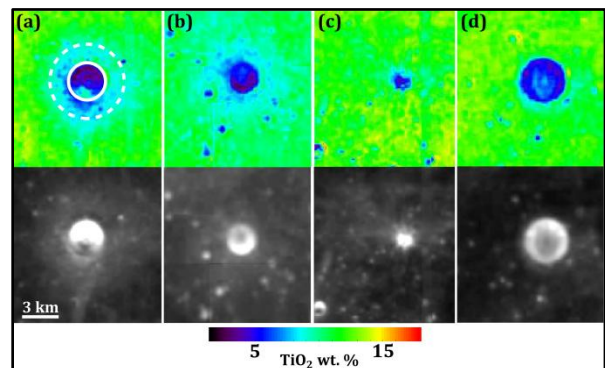
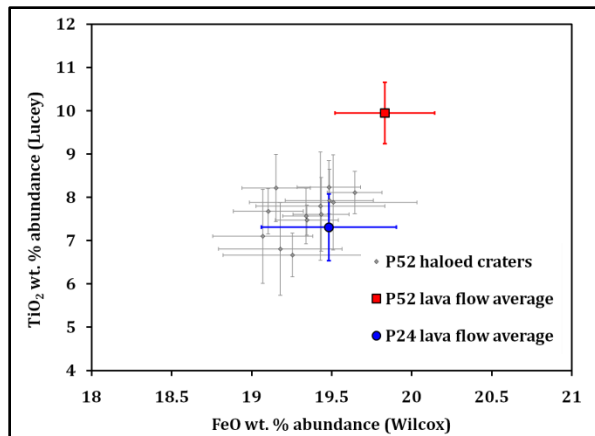


Figure 2. Examples of impact craters within lava flow 'P52' displayed in terms of TiO<sub>2</sub> wt. % [12] and reflectance at 750 nm. The craters in (a) and (b) both possess the TiO<sub>2</sub>-poor (blue) haloes, with (a) displaying bright ejecta and (b) not. The craters in (c) and (d) have no TiO<sub>2</sub>-poor haloes, yet (c) has bright ejecta and (d) does not. The area between the solid (crater rim) and dashed (extent of continuous ejecta) lines in (a) is the region from which data for ejecta compositions were obtained. The ejecta limit does not always completely encompass the halo, but the arbitrary distance of 1 crater radius was chosen for the sake of consistency. The apparently low-TiO<sub>2</sub> crater interior (dark blue) is caused by the bright, non-space weathered material on the steep slopes; asymmetries are caused by variations in illumination due to topography. The scale for all the images is equal.



**Figure 3.** The mean FeO and TiO<sub>2</sub> abundance values (according to [11] and [12] respectively) for the ejecta of the thirteen haloed craters in lava flow ‘P52’, and mean inter-crater values for lava flows ‘P52’ and ‘P24’. Error bars indicate 1 standard deviation of the individual pixel values used to produce the mean values.

We do not attribute the difference in TiO<sub>2</sub> wt. % values for ‘P52’ and the ejecta to an unresolved maturity (albedo) issue as craters both with and without surrounding bright ejecta may or may not display TiO<sub>2</sub>-poor haloes (Fig. 2). Furthermore, on a plot of the 415/750 nm reflectance ratio vs. reflectance at 750 nm (Fig. 4), the ejecta of the haloed craters in lava flow ‘P52’ form a distinct group from the ejecta of a set of craters with no haloes in the same lava flow (the craters with haloes are predominantly larger than those without). The offset of these two groups follows a trend of increased TiO<sub>2</sub> content rather than one of increased maturity and therefore supports the notion that the haloes are indeed caused by lower TiO<sub>2</sub> wt. % contents than their immediate surroundings. Additionally, the two sets of craters display a clear distinction in TiO<sub>2</sub> wt. % values, but not in albedo (both as a function of crater diameter).

This evidence suggests that impact craters within lava flow ‘P52’ have indeed excavated material from a deeper, compositionally different lava flow (i.e. ‘P24’). As such, the diameter of the craters (between ~2 km and ~4 km) can be used estimate their maximum depth of excavation [15, 16], and therefore constrain the thickness of the surficial lava flow. Our results show that the lava flow ‘P24’ lies between ~100 m and ~300 m below the surface of ‘P52’ in this region. This estimate is consistent with previous ones for the total thickness of basalts in this area of ~500 - 1000 m [6-8]. Our estimate for the thickness of ‘P52’ suggests that the two flows, ‘P52’ and ‘P24’, each make up approximately half of the total thickness of basalt.

**Conclusion:** We have identified impact craters within Oceanus Procellarum that have excavated and brought to the surface material from deposits underlying

the surface lava flows. By using crater morphometric relationships, constraints can be placed on the thickness of these uppermost lava flows, as well as for their volumes and eruption rates. These methods allow the study of individual lava flows within a mare region, and thus provide a detailed view of the region’s volcanic history. This type of investigation should be extended (especially using the new, higher spectral and spatial resolution datasets from instruments such as M<sup>3</sup> on Chandrayaan-1 [17]) to cover large areas of the lunar maria and therefore develop our understanding of the Moon’s interior and evolution. Such studies will also highlight areas of particular scientific interest that may be worthy of future human and/or robotic surface exploration and sampling.

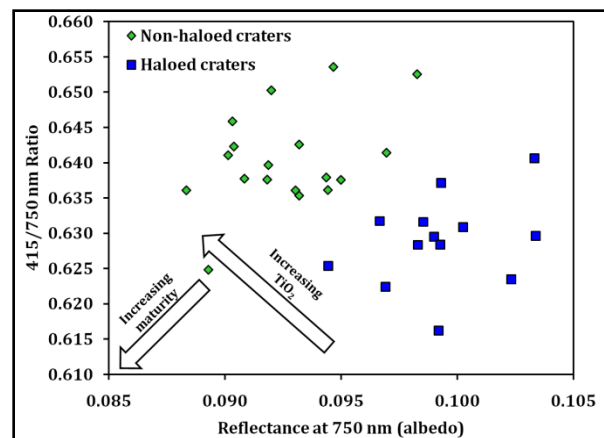


**Figure 4.** 415/750 nm reflectance ratio vs. 750 nm reflectance values for the haloed craters in lava flow ‘P52’ (blue symbols) and several craters in the same lava flow with no observable halo (green symbols). The trend of these two groups follows one for increased TiO<sub>2</sub> rather than increased maturity.

**References:** [1] Hiesinger H. et al. (2000) *JGR*, 105 (E12), 29,239-29,275. [2] Hiesinger H. et al. (2003) *JGR*, 108 (E7), 5065. [3] Carr M.H. (1966) *USGS*, I-489 (LAC-42). [4] McCauley J.F. (1967) *USGS*, I491 (LAC-56). [5] Pieters C.M. (1978) *LPS IX*, 2825-2849. [6] De Hon R.A. (1978) *LPS IX*, 229-231. [7] De Hon R.A. (1979) *LPS X*, 2935-2955. [8] Heather D.J. & Dunkin S.K. (2002) *Planet. Space Sci.* 50, 1299-1309. [9] Ono T. et al. (2009) *Science*, 323, 909-912. [10] Eliason E. et al. (1999) *USGS*, USA\_NASA\_PDS\_CL\_4001-4078. [11] Wilcox B.B. et al (2005) *JGR*, 110, E11001. [12] Lucey P.G. et al. (2000) *JGR*, 105 (E8), 20,297-20,305. [13] Oberbeck V.R. et al. (1974) *LPS V*, 111-136. [14] Moore H.J. (1974) *LPS V*, 71-100. [15] Melosh H.J. (1989) *Impact cratering a geologic process*, OUP. [16] Stöffler D. et al. (2006) *Rev. Min Geochem.*, 60, 519-596. [17] Pieters C. et al. (2009) *Current Science*, 96, 500-505.